

A Novel Method of Nanocontact Fabrication for Andreev Reflection Measurement *

Wang Tianxing¹, Wei Hongxiang¹, Ren Cong¹, Han Xiufeng^{1,†}, Clifford E²,
Langford R M², Bari M A², and Coey J M D²

(1 State Key Laboratory of Magnetism & State Key Laboratory of Superconductors, Institute of Physics,
Chinese Academy of Sciences, Beijing 100080, China)

(2 Department of Physics, Trinity College, Dublin 2, Ireland)

Abstract : A new method of nanocontact fabrication for Andreev reflection measurement based on the nanopore method using a SiN membrane with focused ion beam technique is presented. With this method, controllable, clean, tensionless nano-contacts for spin polarization probing can be obtained. Measurements of the fabricated samples show complicated spectral structures with a zero bias anomaly and dip structures from quasiparticle interactions. A control sample of Co₄₀Fe₄₀B₂₀ is measured with Nb tip method. None of the measured spectra can be explained satisfactorily by present theory. Further analysis of the contact interface and a more complete theory are needed to extract a reliable spin polarization message with the point contact Andreev reflection method.

Key words : point contact Andreev reflection; controllable; spin polarization

PACC : 7550P

CLC number : TN304.7

Document code : A

Article ID : 0253-4177(2006)04-0591-07

1 Introduction

The rapid development of magnetoelectronic devices in recent years is stimulating a search for materials with high spin polarization since the performance of such devices depends critically on a substantial spin polarization^[1~3]. A reliable method for determining the spin polarization (P) of new materials is therefore important.

There are currently only a few methods to determine P . The most widely used method so far involves the use of a superconducting tunnel junction, which consists of a superconductor/insulator/ferromagnet stack of layers^[4,5]. The usual structure is Al/Al₂O₃/other metal. The value of P can be determined by exploiting the characteristics of the density of states of the superconductor in a magnetic field. There are, however, a number of drawbacks in this method. Tunneling occurs only within a few monolayers at the interfaces between

the metal electrodes and the insulating barrier layer^[6]. The spin polarization of these interfacial monolayers can be substantially different from that of the bulk. Furthermore, the fabrication of a pinhole-free insulating barrier layer with a thickness of about 1nm is proved to be rather difficult. The characteristics of the barrier material must also be taken into account in determining P via the tunneling matrix elements.

Recently, there has been a renewed interest in metal/superconductor junctions, largely driven by the ability to measure the spin polarization P of the conduction electrons in a metal with what is called the point-contact Andreev reflection (PCAR) method^[7~9].

Andreev reflection is a process by which an electron, incident from a normal metal on a normal metal/superconductor interface with energy less than the superconductor energy gap (Δ), is converted into a Cooper pair in the superconductor, leaving a hole in the opposite spin band of the met-

* Project supported by the Science Foundation of Ireland, the China-Ireland Science and Technology Collaboration Research Fund Between the Science Foundation of Ireland and the State Key Project of Fundamental Research Ministry of Science and Technology of China (No. 2001CB610601), the National Natural Science Foundation of China (Nos. 10510136, 10574156, and 50271081), and the National Science Fund for Distinguished Young Scholars (Nos. 50325104, 50528101)

† Corresponding author. Email: xfhan@aphy.iphy.ac.cn

Received 28 November 2005, revised manuscript received 25 January 2006

© 2006 Chinese Institute of Electronics

al. The detailed theory—BTK theory—was developed by Blonder *et al.*^[10]. For ferromagnetic materials, the majority and minority bands are not equal, and the Andreev reflection is seriously suppressed^[11].

The spin polarization of a metal is usually defined as

$$P_n = (n_{\uparrow} - n_{\downarrow}) / (n_{\uparrow} + n_{\downarrow})$$

where n_{\uparrow} and n_{\downarrow} are the charge densities at the Fermi energy of the majority and minority bands, respectively. However, in the measurement of spin polarization with the PCAR or tunneling method, one measures $P = (I_{\uparrow} - I_{\downarrow}) / (I_{\uparrow} + I_{\downarrow})$, the imbalance in the currents of the majority and minority carriers^[9]. We will use this definition of P , which is relevant to the spin polarization as measured by PCAR, under certain conditions, such as when the Fermi velocities of all the spin currents are the same, so that $P = P_n$ ^[12]. Note that, although I_{\uparrow} can be larger or smaller than I_{\downarrow} , with PCAR we can only measure the absolute value of the spin polarization $|P|$. PCAR does not suffer from the above mentioned drawbacks since it does not rely on the preparation of a thin insulating barrier layer and it probes the polarization not merely for a few monolayers at the interface but on the length scale of the electron mean free path in the metal. Furthermore, PCAR is very well suited for the measurement of the spin polarization of new materials, for which the fabrication of high quality tunnel junctions is often a formidable challenge.

The most frequently used method recently involves the use of a fine tip of a normal metal (superconductor) controlled by a differential screw. The tip is usually fabricated by chemical etching or by fine mechanical grinding. The tip is then brought into mechanical contact with a superconductor (normal metal) at a certain pressure. This is rather simple compared to the tunneling method and other recent methods, since it is easy to change the material to be measured and the contact resistance is easy to control by adjusting the pressure on the tip. Although it seems a great success to extract information from normal metals and ferromagnetic metals with this method, there are still some drawbacks. The interface at the contact is difficult to control even though the tip is usually ultrasonically cleaned to remove residue. It is also difficult to characterize the contact formed between

the tip and the counter materials. First, the contact area, which is usually calculated by the Sharvin formula^[12,13], cannot be directly controlled. Second, there is a complicated interface with an unclear barrier possibly from residue and oxidation at the contact. Third, there is also tension between the tip and the substrate from a crystal lattice mismatch at the interface and especially from the pressure exerted by the screw, which changes the band structure of the material at the contact. These conditions are very difficult to account for in theory, and they make the barrier parameter Z ^[10] unclear. These problems make the reliability of the extracted spin polarization values doubtful. The importance of the influence of the pressure on the spectrum from the aberrance of the crystal lattice is still unclear at present, so it is not surprising that different experiments give different results^[18,9,14,15]. Therefore a natural, clean contact in such measurements is required.

1] In 1998, Upadhyay *et al.*^[8] used another method to form a natural contact. They fabricated bimetallic nanocontacts by thermal evaporation in a vacuum of 1.33×10^{-5} Pa onto both sides of a silicon-nitride membrane containing a tapered hole made by electron beam lithography (EBL) and reactive ion etching (RIE)^[16]. This is a rather complicated fabrication process, and the measured spectra show obvious barrier characteristics possibly due to the poor quality of the evaporated film.

Recently, focused ion beam (FIB) etching, which makes the fabrication of nanostructures less than 30nm easy, has become a popular nanofabrication technique. We try to form a small hole by this method and then deposit superconducting and other materials on both sides of the membrane with high vacuum magnetron sputtering to form a small metallic contact. With this method, the contact size is determined by the hole size at the contact, which is determined by the parameters of the FIB etching. The contact is then formed naturally by depositing a film at the atomic level at a depositing rate below 0.1nm/s. The contact should be tensionless and clean if there had been no vacuum break. Compared to the bowl-shaped hole by Upadhyay *et al.*^[8], these ion-beam-milled holes have a rather sharp shape.

2 Sample fabrication

100nm thick silicon nitride membranes with silicon-supported frames were used. Nanopores through the silicon nitride membranes were milled using a beam current of 10pA at 30keV. The shape of the pore and the nanocontact size on the under-side of the membrane were determined by FIB cross-sectioning and SEM imaging. If the initial hole diameter was 40nm or less, conical pores were created and the size of the nanocontacts was 3nm or less. If the milled holes were larger than 100nm, then the pores had near-vertical side walls. The conical shape of the 40nm holes was due to the re-deposition of sputtered material onto the sidewalls of the pores during the milling. As the depth of the milled hole increased, the solid angle through which the sputtered material could “escape” decreased, and material was redeposited onto the sidewalls of the hole. Figure 1 shows an SEM image of a FIB-prepared cross-section through a nanopore with a conical shape (in this example the hole was milled to 70nm to yield a wider pore in order to increase the probability of it being cross-sectioned through its centre).

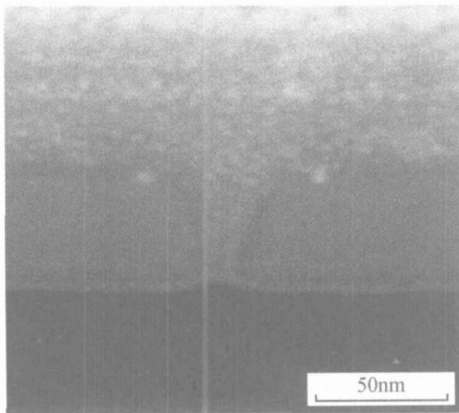


Fig. 1 Cross section of hole filled by sputtering

The nanocontacts were then prepared by sputtering a 100nm thick *s*-wave superconducting film on one side of the silicon nitride membrane and then depositing other normal metal or ferromagnetic materials on the other side after flipping the membrane. To prevent a short between the top and bottom electrodes, the edges were masked

with copper tape during sputtering. To avoid an oxide layer formed when flipping the membrane in the air, the membrane was cleaned by Ar ion etching before depositing the material on other side of it.

3 Results and discussion

In connection with the BTK formalism, there is a difference between ballistic and diffusive transport, defined by the ratio of the mean free path *l* of the electrons and the contact diameter *d*. In general, there are three possible types of transport in a PCAR experiment: ballistic ($l \ll d$), diffusive ($l \gg d$), and intermediate ($l \sim d$).

The diameter of the contact *d* can be calculated from the equation for the junction (contact) resistance^[13,17]

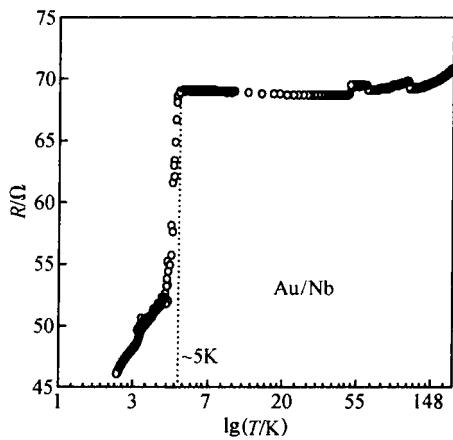
$$R_N = R_0 (1 + Z^2) \quad (4 \quad 1/3 \quad d^2 + /2 d) (1 + Z^2)$$

where the first term in the expression for R_0 is Sharvin resistance for a metallic contact with no barrier^[13,14] for ballistic contacts, while the second is the Maxwell resistance for diffusive transport, where σ is the conductance of the material, and *Z* is the barrier strength of the point contact.

For our metal contacts, the *Z* value is usually very small (< 0.1). We can use the Sharvin resistance to get a rough value of the diameter of the contact. The holes are usually around 10nm in the SEM image, and the resistance of contact is 30 ~ 50 Ω , consistent with the Sharvin formula calculation. Thus the contact should be around 30nm, which is in the ballistic range for Nb, and a little shorter in the film than in the bulk material. There is no great difference between the spin polarizations extracted with ballistic model and diffusive model^[18].

The samples were measured using the standard four-terminal lock-in technique to get the differential resistance dV/dI versus *I* of the point contact. The dV/dI curves were then converted into the dynamical conductance dI/dV -*V* curves, and the normalized conductance curves were obtained by dividing dI/dV -*V* by one of its high bias values. Figure 2 is a typical *R*-*T* curve of an Au/Nb contact, similar to those of the other samples.

For comparison to other works^[8,9,14], Figure 3 shows the dip structures at the (Au/Nb) contact or outside the gap energy range, which are similar to

Fig. 2 R - T curve of Au/Nb

the spectra measured by Sheet *et al.*^[15]. Furthermore, all the spectra show a ZBA structure, which is prominent for normal metal and slight for ferromagnetic metal and the alloy $\text{Co}_{40}\text{Fe}_{48}\text{B}_{12}$. For the Au/Nb sample, there are strong oscillation structures outside the dip structure, and slight ones for Cu/Nb. For ferromagnetic materials, such structures do not appear, but the position of the dip structure is extremely far from the energy of the superconductor gap. The Andreev-reflection-like peak in the Cu/Nb junction is slightly greater than 2, which is similar to the cases in Shan's work^[19]. These features are not presently included in the standard and extended BTK theories^[10,14,20], and the reason for them is still not clear.

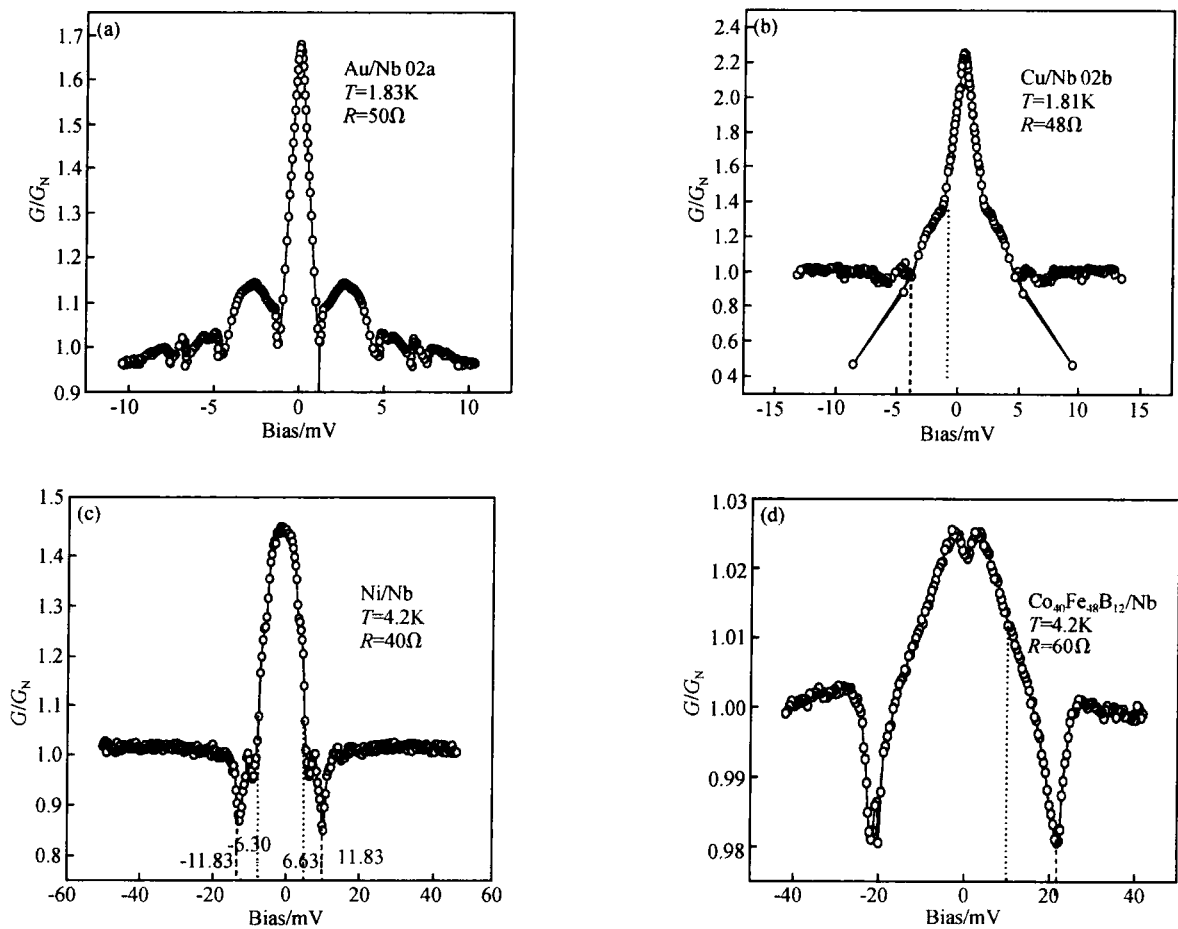


Fig. 3 (a) Normalized GV curve of Au/Nb contact; (b) Normalized GV curve of Cu/Nb contact; (c) Normalized GV curve of Ni/Nb contact; (d) Normalized GV curve of $\text{Co}_{40}\text{Fe}_{48}\text{B}_{12}/\text{Nb}$ contact

There are many possible explanations^[14,15,19], so it is difficult to extract reliable information from them. Qualitatively, the normal metal Au, Cu junc-

tion shows an enhanced conductance within the gap of the superconductor. The conductance of the Ni/Nb, $\text{Co}_{40}\text{Fe}_{48}\text{B}_{12}/\text{Nb}$ junction is depressed within

the gap energy of Nb compared with Au and Cu, especially for $\text{Co}_{40}\text{Fe}_{48}\text{B}_{12}$. Namely, $\text{Co}_{40}\text{Fe}_{48}\text{B}_{12}$ has a high spin polarization, at least as compared with Ni by the PCAR theory.

Sheet *et al.* explained the dip structures by a critical current^[15], and they excluded the proximity effect^[14] as a possible reason that the ferromagnetic material should be a strong pair breaker. For our sample, the dip structures cannot have any correspondence with the superconductor gap except for the Au/Nb case, and the contact size is not in the diffusive range as well, so there must be another reason for these characteristics.

Shan *et al.*^[19] introduced a Josephson junction in series with a normal-metal/ superconductor (N/S) point contact to model the tunneling. By tuning the weights of the point contact Andreev reflection voltage and the Josephson voltage, they obtained results consistent with BCS s -wave pairing in MgC-Ni_3 . Chainani *et al.*^[21] used high sensitivity angle-integrated photoemission spectra for strong-coupling superconductors Pb and Nb. They found a large spectra weight redistribution up to 15meV, which is much larger than the gap energy or T_c of Nb. By estimating the values of the gap using Dynes' function^[22] fit by introducing the thermal broadening parameter due to the finite life of the quasiparticles at the gap edge, they obtain a value of $2(0)/K_B T_c$ for Nb of 3.7, which is in good agreement with the thermodynamic measurement of 3.8, which is a possible reason for the nature of the spectra we obtained.

There are many possible sources for ZBCP, including Kondo-type scattering by magnetic impurities in the small barrier at the interface^[23-26], Cooper pair or reflectionless tunneling in high-transmittance junctions^[27,28], and anomalies in tunneling between two 2D electron gases^[29,30].

For comparison, Figure 4 gives the Andreev spectrum of a $\text{Co}_{40}\text{Fe}_{40}\text{B}_{20}/\text{Nb}$ contact made simply by applying an Nb tip. The solid line is a BTK fit with parameters $T = 2\text{K}$, $\Delta = 1.225\text{meV}$, and $Z = 0.03$. The significant broadening is due to a large thermal broadening effect, which is always observable in point contact measurements, but there is no obvious ZBA structure or dip structure. From the fit, we obtain a polarization of 0.455, smaller than that from the tunneling junction value obtained by the Jullière formula^[31], which is about 0.6 ~ 0.7.

Therefore further verification is needed.

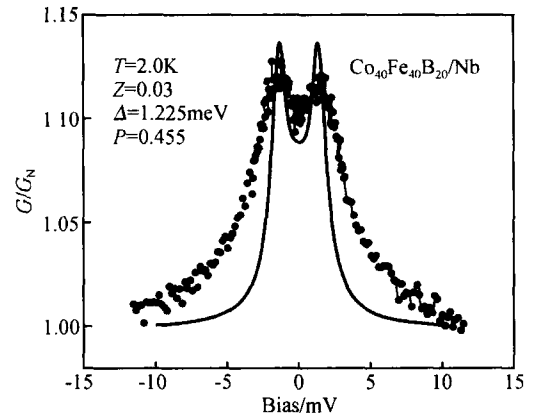


Fig. 4 Normalized G/V curve of $\text{Co}_{40}\text{Fe}_{40}\text{B}_{20}/\text{Nb}$ contact by Nb tip method. The straight line is the BTK fit. For thermal broadening of the spectrum, only the key feature of the gap structure is fitted by $T = 2\text{K}$, $\Delta = 1.225\text{meV}$, $Z = 0.03$.

From our work and other works^[15], the ZBA usually appears accompanied by the dip structure for junctions with low temperature superconductors^[15,19]. Most likely, they come from the same source. For our sputtered samples, the possible mixing of different materials from the roughness at the contact may be one reason. Ni and CoFeB are not simple Stoner ferromagnets; their band structure is quite complicated, and a complete theory should take the s and d -band electrons, and their hybridization into account. For reliable extraction of spin polarization information from these materials, not only a high transparency and clean contact are needed, but also a more delicate theory including possible mechanisms.

4 Conclusion

A new method for fabricating Andreev nanocontacts involving the FIB etching of a membrane is used for spin polarization measurements. With this simple method, we can get a controllable, clean, tensionless interface at the contact. The spectra measured from normal metal and ferromagnetic metal showed complicated peak structures possibly from ZBA and quasiparticle interactions for all membrane samples. For the ferromagnet/Nb junctions, the gap structures are smeared. The present standard and extended BTK theories cannot extract the spin polarization reliably. Another ferromagnetic $\text{Co}_{40}\text{Fe}_{40}\text{B}_{20}$ sample is measured by

an Nb tip, for which the dip structure cannot be observed and the spectrum is thermally broadened, possibly by the diffusive transport. Therefore, to get reliable spin polarization information by the PCAR method, not only a smooth, sharp, ballistic contact, but also an improved theory that includes real material-related mechanisms is needed.

References

- [1] Prinz G A. Spin-polarized electron transport. *Phys Today*, 1995, 48(4):58
- [2] Daughton J M, Pohm A V, Fayfield R T, et al. Applications of spin dependent transport materials. *J Phys D*, 1999, 32:R169
- [3] Wei Shuyi, Yan Yuli, Wang Tianxing, et al. Magnetism and stability of diluted magnetic semiconductor ($\text{Ga}_{1-x}\text{Fe}_x$). *As. Chinese Journal of Semiconductors*, 2004, 25(12):1586
- [4] Meservey R, Tedrow P M. Spin-polarized electron tunneling. *Phys Rep*, 1994, 238:173
- [5] Monsma D J, Parkin S S P. Temporal evolution of spin-polarization in ferromagnetic tunnel junctions. *Appl Phys Lett*, 2000, 77:720
- [6] Leclair P, Swagten H J M, Köhlhepp J T, et al. Apparent spin polarization decay in Cu-dusted $\text{Co}/\text{Al}_2\text{O}_3/\text{Co}$ tunnel junctions. *Phys Rev Lett*, 2000, 84:2933
- [7] De Jong M J M, Beenakker C W J. Andreev reflection in ferromagnet-superconductor junctions. *Phys Rev Lett*, 1995, 74:1657
- [8] Upadhyay S K, Palanisamai A, Louie R N, et al. Probing ferromagnets with Andreev reflection. *Phys Rev Lett*, 1998, 81:3247
- [9] Soulen R J, Byers J M, Osofsky M S, et al. Measuring the spin polarization of a metal with a superconducting point contact. *Science*, 1998, 282:85
- [10] Blonder G E, Tinkham M, Klapwijk T M. Transition from metallic to tunneling regimes in superconducting microconstrictions: excess current, charge imbalance, and supercurrent conversion. *Phys Rev B*, 1982, 25:4515
- [11] Mazin I I. How to define and calculate the degree of spin polarization in ferromagnets. *Phys Rev Lett*, 1999, 83:1427
- [12] Sharvin Y V. A possible method for studying Fermi surfaces. *Zh Eksp Teor Fiz*, 1965, 48:984 [*Sov Phys JETP*, 1965, 21:655]
- [13] Jansen A G M, van Gelder A P, Wyder P. Point-contact spectroscopy in metals. *J Phys C*, 1980, 13:607
- [14] Strijkers G J, Ji Y, Yang F Y, et al. Andreev reflections at metal/superconductor point contacts: measurement and analysis. *Phys Rev B*, 2001, 63:104510
- [15] Sheet G, Mukhopadhyay S, Raychaudhuri P. Role of critical current on the point-contact Andreev reflection spectra between a normal metal and a superconductor. *Phys Rev B*, 2004, 69:134507
- [16] Ralls K S, Buhrman R A, Tiberio R C. Fabrication of thin-film metal nanobridges. *Appl Phys Lett*, 1989, 55:2459
- [17] Nolic B K, Allen P B. Electron transport through a circular constriction. *Phys Rev B*, 1999, 60:3963
- [18] Woods G T, Woods G T, Soulen R J, et al. Analysis of point-contact Andreev reflection spectra in spin polarization measurements. *Phys Rev B*, 2004, 70:054416
- [19] Shan L, Tao H J, Gao H, et al. s -wave pairing in MgCNi_3 revealed by point contact tunneling. *Phys Rev B*, 2003, 68:144510
- [20] Mazin I I, Golubov A A, Nadgorny B. Probing spin polarization with Andreev reflection: a theoretical basis. *J Appl Phys*, 2001, 89:7576
- [21] Chainani A, Yokoya T, Kiss T, et al. Photoemission spectroscopy of the strong-coupling superconducting transitions in lead and niobium. *Phys Rev Lett*, 2000, 85:1966
- [22] Dynes R C, Narayanamurti V, Garno J P. Direct measurement of quasiparticle-lifetime broadening in a strong-coupled superconductor. *Phys Rev Lett*, 1978, 41:1509
- [23] Laube F, Goll G, Löhneysen H V, et al. Spin-triplet superconductivity in Sr_2RuO_4 probed by Andreev reflection. *Phys Rev Lett*, 2000, 84:1595
- [24] Greene L H, Covington M, Aprili M, et al. Observation of broken time-reversal symmetry with Andreev bound state tunneling spectroscopy. *Phys B*, 2000, 280:159
- [25] Shen L Y L, Rowell J M. Zero-bias tunneling anomalies-temperature, voltage, and magnetic field dependence. *Phys Rev*, 1968, 165:566
- [26] Wolf E L, Losee D L. Spectroscopy of kondo and spin-flip scattering: high-field tunneling studies of Schottky-barrier junctions. *Phys Rev B*, 1970, 2:3660
- [27] Kastalsky A, Kleinsasser A W, Greene L H, et al. Observation of pair currents in superconductor-semiconductor contacts. *Phys Rev Lett*, 1991, 67:3026
- [28] Beenakker C W J, van Houten H. Josephson current through a superconducting quantum point contact shorter than the coherence length. *Phys Rev Lett*, 1991, 66:3056
- [29] Ashoori R C, Lebens J A, Bigelow N P, et al. Equilibrium tunneling from the two-dimensional electron gas in GaAs: evidence for a magnetic-field-induced energy gap. *Phys Rev Lett*, 1990, 64:681
- [30] Eisenstein J P, Pfeiffer L N, West K W. Coulomb barrier to tunneling between parallel two-dimensional electron systems. *Phys Rev Lett*, 1992, 69:3804
- [31] Jullière M. Tunneling between ferromagnetic films. *Phys Lett*, 1975, 54A:225

一种用于制备安德鲁反射样品的新方法*

王天兴¹ 魏红祥¹ 任 聪¹ 韩秀峰^{1,†} Clifford E² Langford R M² Bari M A² Coey J M D²

(1 中国科学院物理研究所 磁学国家重点实验室, 超导国家重点实验室, 北京 100080)

(2 圣三一学院物理系, 都柏林 2, 爱尔兰)

摘要: 提供了一种用于安德鲁反射测量样品制备新方法. 该方法采用聚焦粒子束刻蚀和磁控溅射, 可以获得可控的、干净的、无应力的纳米接触用于自旋极化探测. 所制备的样品中, 磁性和非磁性材料样品的反射谱都表现出复杂的峰和谷结构, 这些结构可能源于与界面相关的零偏压反常以及与激发态相关的准离子相互作用. 对另一个 $\text{Co}_{40}\text{Fe}_{40}\text{B}_{20}$ 合金样品采用简单的钨针尖压针方法进行了对比性测量, 反射谱中没有观察到谷结构, 但谱结构出现较明显的热扩展, 这种热扩展可能来源于界面处的非弹性输运. 所有的反射谱目前还不能由现有的理论给出令人满意的解释. 利用点接触反射方法获得可靠的自旋极化信息还有赖于接触界面特征的进一步分析. 而一个更切合实际的、更完善的理论成为迫切的需要.

关键词: 点接触安德鲁反射; 可控的; 自旋极化

PACC: 7550P

中图分类号: TN304.7

文献标识码: A

文章编号: 0253-4177(2006)04-0591-07

* 爱尔兰科学基金, 爱尔兰科学基金会和中国科学技术部国家重点项目基础研究部的中爱科学技术合作基金(批准号: 2001CB610601), 国家自然科学基金(批准号: 10610136, 10574156, 50271081) 及国家杰出青年基金(批准号: 50325104, 50528101) 资助项目

† 通信作者. Email: xfhan@aphy.iphy.ac.cn

2005-11-28 收到, 2006-01-25 定稿